AFRL-RY-WP-TP-2011-1001

MODELING AND DIRECT ELECTRIC-FIELD MEASUREMENTS OF PASSIVELY MODE-LOCKED QUANTUM-DOT LASERS (POSTPRINT)

Nicholas G. Usechak and Vassilios Kovanis

Electro-optic Components Technology Branch
Aerospace Components Division

Yongchun Xin, Chang-Yi Lin, and Luke F. Lester

University of New Mexico

Daniel J. Kane

Southwest Sciences, Inc.

JULY 2010

AIR FORCE RESEARCH LABORATORY
SENSORS DIRECTORATE
WRIGHT-PATTERSON AIR FORCE BASE, OH 45433-7320
AIR FORCE MATERIEL COMMAND
UNITED STATES AIR FORCE

REPORT DOCUMENTATION PAGE

Form Approved
OMB No. 0704-0188

1. REPORT DATE *(DD-MM-YY)*	2. REPORT TYPE	3. DATES COVERED *(From - To)*
July 2010	Journal Article Postprint	15 September 2008 – 31 July 2010

4. TITLE AND SUBTITLE
MODELING AND DIRECT ELECTRIC-FIELD MEASUREMENTS OF PASSIVELY MODE-LOCKED QUANTUM-DOT LASERS (POSTPRINT)

5a. CONTRACT NUMBER
FA8650-07-M-1182

5b. GRANT NUMBER

5c. PROGRAM ELEMENT NUMBER
65502F

6. AUTHOR(S)
Nicholas G. Usechak and Vassilios Kovanis (AFRL/RYDP)
Yongchun Xin, Chang-Yi Lin, and Luke F. Lester (University of New Mexico)
Daniel J. Kane (Southwest Sciences, Inc.)

5d. PROJECT NUMBER
3005

5e. TASK NUMBER
13

5f. WORK UNIT NUMBER
300513M8

7. PERFORMING ORGANIZATION NAME(S) AND ADDRESS(ES)
Electro-optic Components Technology Branch (AFRL/RYDP)
Aerospace Components Division
Air Force Research Laboratory, Sensors Directorate
Wright-Patterson Air Force Base, OH 45433-7320
Air Force Materiel Command, United States Air Force

University of New Mexico
Center for High Technology Materials
Albuquerque, NM 87106

Southwest Sciences, Inc.
Santa Fe, NM 87505

8. PERFORMING ORGANIZATION REPORT NUMBER

9. SPONSORING/MONITORING AGENCY NAME(S) AND ADDRESS(ES)
Air Force Research Laboratory
Sensors Directorate
Wright-Patterson Air Force Base, OH 45433-7320
Air Force Materiel Command
United States Air Force

10. SPONSORING/MONITORING AGENCY ACRONYM(S)
AFRL/RYDP

11. SPONSORING/MONITORING AGENCY REPORT NUMBER(S)
AFRL-RY-WP-TP-2011-1001

12. DISTRIBUTION/AVAILABILITY STATEMENT
Approved for public release; distribution unlimited.

13. SUPPLEMENTARY NOTES
Paper contains color. Journal article published in *IEEE Journal of Selected Topics in Quantum Electronics*, Vol. 15, No. 3, May/June 2009.

This work is one of a number of manuscripts published in peer-reviewed journals as a result of in-house work on technical report AFRL-RY-WP-TR-2010-1195.

14. ABSTRACT
A delay differential equation model of a passively mode-locked two-section quantum-dot laser reveals pulse asymmetry that is experimentally confirmed through direct electric-field measurements using frequency-resolved optical gating. This finding indicates that conventional autocorrelators, which obscure the underlying pulse structure due to the symmetry inherent in autocorrelation, are of limited utility in the characterization of these lasers.

15. SUBJECT TERMS
delay differential equations (DDEs), mode-locked semiconductor lasers, quantum-dot lasers

16. SECURITY CLASSIFICATION OF:			17. LIMITATION OF ABSTRACT:	18. NUMBER OF PAGES	19a. NAME OF RESPONSIBLE PERSON (Monitor)
a. REPORT	b. ABSTRACT	c. THIS PAGE			Nicholas G. Usechak
Unclassified	Unclassified	Unclassified	SAR	14	19b. TELEPHONE NUMBER *(Include Area Code)* N/A

Modeling and Direct Electric-Field Measurements of Passively Mode-Locked Quantum-Dot Lasers

Nicholas G. Usechak, *Member, IEEE*, Yongchun Xin, *Member, IEEE*, Chang-Yi Lin, *Student Member, IEEE*, Luke F. Lester, *Senior Member, IEEE*, Daniel J. Kane, *Member, IEEE*, and Vassilios Kovanis

***Abstract*—A delay differential equation model of a passively mode-locked two-section quantum-dot laser reveals pulse asymmetry that is experimentally confirmed through direct electric-field measurements using frequency-resolved optical gating. This finding indicates that conventional autocorrelators, which obscure the underlying pulse structure due to the symmetry inherent in autocorrelation, are of limited utility in the characterization of these lasers.**

***Index Terms*—Delay differential equations (DDEs), mode-locked semiconductor lasers, quantum-dot lasers.**

I. Introduction

QUANTUM-DOT lasers have been the focus of considerable excitement in recent years due to their low threshold currents [1], ease of mode locking [2], low linewidth enhancement factors [3], and temperature insensitivity [4]. They hold promise as compact and robust amplifiers, continuous-wave (CW) lasers, and mode-locked lasers. Moreover, they have even recently been used as building blocks in optical switches [5] indicating the role they may play in device integration. These lasers may also prove useful in applications that require a train of stable pulses such as clocks for computers and video game systems. In comparison with quantum-well lasers, quantum-dot lasers have shown themselves to mode-lock more easily, which hints at an underlying robustness that should also lead to improved environmental stability [6], [7].

Despite the progress made to fully understand these lasers, there are still obstacles that need to be overcome, for example, resolving issues surrounding the measurement of the linewidth enhancement factor [8]. The focus of this paper is another area that warrants improvement: the exclusive use of autocorrelation to characterize the mode-locked pulses generated by these devices. For the purpose of improving understanding and comparing with models, autocorrelation should be augmented by a full electric-field characterization, a matter that has gone largely unnoticed in the quantum-dot laser community until recently [9], [10]. Although autocorrelation provides a rough estimate of pulsewidth, it offers no real insight into pulse shape. Nevertheless, the straightforward sounding task of measuring the electric field directly from a mode-locked semiconductor laser is frustrated by the low peak powers ($\lesssim$1 W) routinely generated by these devices. Low power levels can make autocorrelation itself difficult due to the weak nonlinear conversion efficiencies that accompany them. Therefore, electric-field measurement approaches, which rely on spectrally resolving the nonlinear autocorrelation signal, suffer an additional SNR degradation at low power levels limiting the utility of off-the-shelf commercial systems. One convenient solution is to amplify the output of the laser using a semiconductor optical amplifier (SOA) [11]; however, SOA's add chirp and distort the pulse properties especially when working with short ($\lesssim$1 ps), broadband, or heavily chirped pulses.

In Section II, we begin our investigation of the shape of a mode-locked pulse by using a reduced system of equations governing the optical field and the carriers in a gain/absorber region of a generic two-section laser. These equations are then simplified through a Galilean transformation, normalization, and the application of the laser's periodic boundary condition to reduce the system of partial differential equations (PDEs) into a system of delay differential equations (DDEs). Section III consists of an investigation of the optical pulses produced by this model. One of the main findings of this section is that, in general, the mode-locked pulses possess asymmetry. In this section, we also introduced an ansatz to use for fitting the pulse shape that agrees well with the results of the model. Section IV describes the fabrication and packaging of the quantum-dot laser used to experimentally investigate the mode-locked pulse shape and our experimental setup. The laser was characterized by measuring its optical spectrum, the optical autocorrelation signal, and the microwave spectrum, as discussed in Section V. Meanwhile, a highly sensitive frequency-resolved optical gating (FROG) device was built and the pulse structure was more carefully investigated using this system. Finally, the model, analytic fit, and experimentally extracted optical field are compared before concluding remarks are given. Our conclusions are summarized in Section VI.

Manuscript received October 31, 2008; revised December 2, 2008. First published February 27, 2009; current version published June 5, 2009. This work was supported by the Air Force Research Laboratory (AFRL) Small Business Innovation Research (SBIR) Number FA8650-07-M1182 and by the Air Force Office of Scientific Research (AFOSR) under Contract LRIR 09RY04COR.

N. G. Usechak and V. Kovanis are with the Air Force Research Laboratory, Wright–Patterson Air Force Base (AFB), Dayton, OH 45433 USA (e-mail: nicholas.usechak@us.af.mil; vassilios.kovanis@us.af.mil).

Y. Xin was with the Center for High Technology Materials, University of New Mexico, Albuquerque, NM 87106 USA. He is now with IBM Systems and Technology Group, Semiconductor Solutions, Armonk, NY 10504-1722 USA (e-mail: yxin@us.ibm.com).

C.-Y. Lin and L. F. Lester are with the Center for High Technology Materials, University of New Mexico, Albuquerque, NM 87106 USA (e-mail: cylin@unm.edu; luke@chtm.unm.edu).

D. J. Kane is with Southwest Sciences, Inc., Santa Fe, NM 87505 USA (e-mail: djkane@swsciences.com).

Color versions of one or more of the figures in this paper are available online at http://ieeexplore.ieee.org.

Digital Object Identifier 10.1109/JSTQE.2008.2012268

II. Model

Considerable effort has been devoted to the modeling of mode-locked semiconductor lasers. Nevertheless, the different dimensionality of quantum-dot media opens up the possibility that these lasers exhibit different microscopic properties than quantum-well lasers. This could result from markedly different values for operating parameters such as the linewidth enhancement factor [3]. Of greater interest would be the erroneous treatment of presumably "constant" terms as constants, when they actually have a pronounced nonlinear dependance that must be accounted for [8]. These issues are still under investigation and are best determined through careful experimental work coupled with numerical simulations.

In this paper, we restrict our attention to seeking a simple macroscopic model of a two-section mode-locked quantum-dot laser able to capture the salient features with the objective of comparing with experiential results. We begin with a generic system of PDEs that govern the evolution of the optical field and the carriers in the gain (k = g) and saturable absorber (k = abs) sections of any two-section semiconductor laser

$$\frac{\partial E(t,z)}{\partial z} = -\frac{1}{\nu}\frac{\partial E(t,z)}{\partial t} + \frac{g_{\rm k}\Gamma_{\rm k}}{2}\left(1 - i\alpha_{\rm k}\right)\left[N_{\rm k}(t,z) - N_{\rm k}^{\rm tr}\right]E(t,z) \quad (1)$$

$$\frac{\partial N_{\rm k}(t,z)}{\partial t} = J_{\rm k} - \frac{N_{\rm k}(t,z)}{\tau_{\rm k}} - \nu g_{\rm k}\Gamma_{\rm k}\left[N_{\rm k}(t,z) - N_{\rm k}^{\rm tr}\right]|E(t,z)|^2. \quad (2)$$

Equation (1) describes the effect of propagation on a slowly varying electric field $E(t,z)$ inside the semiconductor where it has been assumed that dispersive and nonlinear effects are negligible. The group velocity dispersion ν is assumed to be constant in the gain and absorber sections while the gain/loss $g_{\rm k}$, confinement factors $\Gamma_{\rm k}$, and linewidth enhancement factors $\alpha_{\rm k}$ are assumed to differ. This rate equation model assumes charge neutrality leaving us to keep track only of electron carrier densities $N_{\rm k}(t,z)$ and their threshold values $N_{\rm k}^{\rm tr}$ in (2). Equation (2) also accounts for injected current J_k and the carrier lifetimes τ_k in each section. To complete the model, it is assumed that spectral filtering can be treated as a lumped parameter located at one of the facets of the laser without compromising accuracy.

If it is assumed that the gain spectrum is symmetric, that negligible intracavity pulse breathing exists, and that the lumped filtering and (1) and (2) form an accurate model for the laser, the laser's periodic boundary condition can be used to reduce the coupled PDE system into a nonlinear DDE system [12], [13]. DDEs have only recently been applied to mode-locked lasers [12]; however, they have been used extensively in other areas of optics, in particular, to describe feedback instabilities in semiconductor lasers [14] as well as passive optical devices [15] for the past three decades. During this time, they have enjoyed a substantial level of success in modeling observed experimental behavior.

Our treatment follows from the work of Vladimirov and Turaev [12], [13] in which (1) and (2) are simplified through a coordinate transformation to a moving time frame τ that has been normalized to the carrier lifetime in the saturable absorber $\tau_{\rm abs}$. Integrals are then performed on the system of normalized PDEs to remove the spatial dependence of the carriers and ultimately obtain a system of DDEs [12], [13]. This introduces a new set of terms that are functions of only time for the carriers in the gain media G, the carriers in the absorber Q, and the optical field A; these terms are governed by [13]

TABLE I
Parameter Values Used in Numerical Simulations

$T = 1.5$	$g_0 = 2.0$	$q_0 = 4.0$
$\alpha_{\rm g} = 2.0$	$\alpha_{\rm abs} = 2.3$	$\Gamma = 1.3 \times 10^{-2}$
$s = 27.25$	$\gamma = 53.3$	$\kappa = 0.15$

$$\frac{dA(\tau)}{d\tau} = \gamma\sqrt{\kappa}\exp\left[\frac{1}{2}(1 - i\alpha_{\rm g})G(\tau - T) - \frac{1}{2}(1 - i\alpha_{\rm abs})Q(\tau - T)\right]A(\tau - T) - \gamma A(\tau) \quad (3)$$

$$\frac{dG(\tau)}{d\tau} = g_0 - \Gamma G(\tau) - e^{-Q(\tau)}(e^{G(\tau)} - 1)|A(\tau)|^2 \quad (4)$$

$$\frac{dQ(\tau)}{d\tau} = q_0 - Q(\tau) - s(1 - e^{-Q(\tau)})|A(\tau)|^2. \quad (5)$$

In these equations, γ incorporates the effect of spectral filtering, $\alpha_{\rm g}$ and $\alpha_{\rm abs}$ are the linewidth enhancement factors in the gain and absorber media, respectively, and κ accounts for linear cavity losses. DDEs incorporate history that shows up in (3) through the evaluation of the optical field A, gain carrier density G, and absorber carrier density Q at the times $\tau - T$, where T is the normalized round-trip time. $\Gamma = \tau_{\rm abs}/\tau_{\rm g}$ is the ratio between the gain and absorber relaxation times and $s = g_{\rm abs}/g_{\rm g}$ is a ratio between the gain and loss coefficients in the separate media. Finally, g_0 and q_0 are gain and absorption parameters obtained by spatially integrating over the normalized currents in each section.

Equations (3)–(5) were derived directly from (1) and (2) and as such are applicable to any laser governed by these equations as long as the approximations made remain reasonable. In quantum-dot lasers containing wetting layers, a more thorough treatment for the carriers has been investigated using a rate equation approach [16] and through the introduction of an additional set of carrier equations in a DDE system [17]. The devices investigated in this paper did not contain wetting layers, and for the reasons noted in the end of Section V, we did not pursue such a model.

III. Numerical Results

The performance of a laser suitably described by (1) and (2) is now investigated through the DDE model of (3)–(5) using the judiciously chosen values given in Table I. To provide an overview of the parameter space, Fig. 1 summarizes the stability of the pulse trains about a fixed set of parameters. In this case, all extrema of the magnitude of the optical field have been plotted over 20 round-trips well after convergence was found while

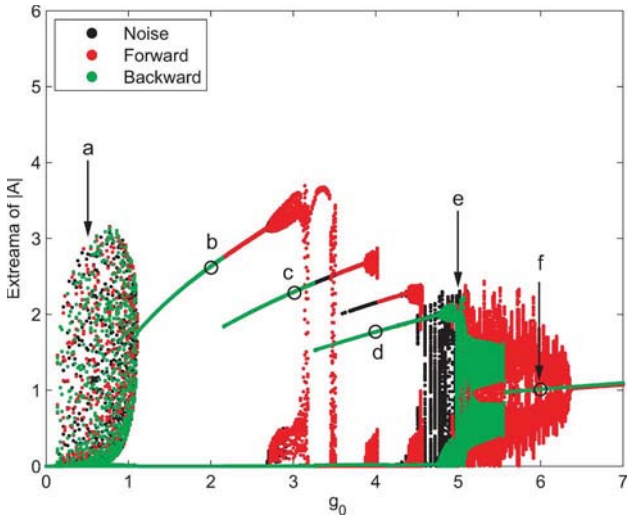

Fig. 1. Bifurcation diagram shows different regimes of operation for this laser as a function of the gain parameter. In this case, the figure predicts the following states: below threshold, Q-switched mode locking, stable mode locking with one, two, three, and four pulses, a region of noisy oscillation, and a CW operation. The gray scale (color online) of the points indicates whether they were generated by seeding the simulation with noise or the result of a previous simulation with a smaller (forward) or larger (backward) gain value. The parameter values used to generate the figure are given in Table I. The y-axis plots the magnitude of the field to simplify comparison with Fig. 2.

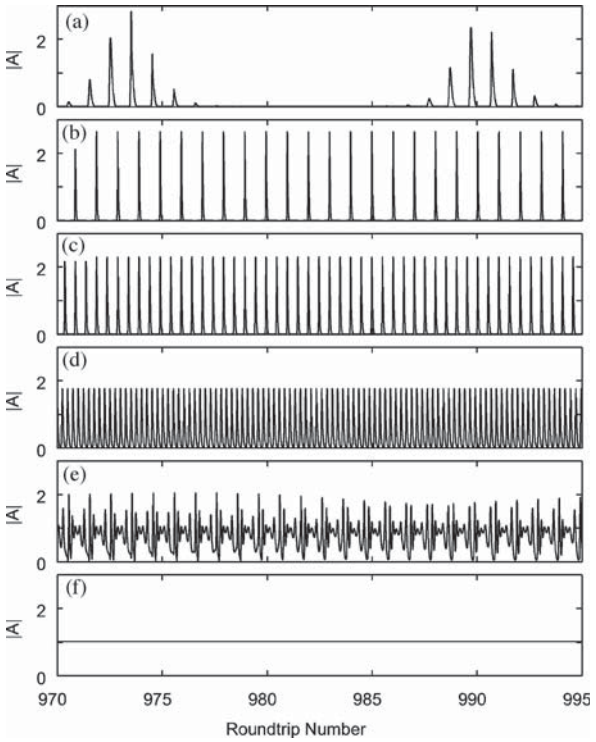

Fig. 2. Optical pulse train taken from specific points in the bifurcation diagram of Fig. 1 to illustrate the different regions of operation. (a) Q-switched mode locking ($g_0 = 0.5$). (b) Fundamental mode locking ($g_0 = 2.0$). (c) Mode locking with two pulses ($g_0 = 3.0$). (d) Mode locking with four pulses ($g_0 = 4.0$). (e) Oscillation ($g_0 = 5.0$). (f) CW output ($g_0 = 6.0$). The y-axis plots the magnitude of the field (not intensity) in order to facilitate comparison between the different subfigures while using the same axis scale.

the value of the gain term g_0 is varied to indicate its role on performance.

This figure provides a simple way to identify different operating domains, for example, five distinct regions are identified. Fig. 1 also provides an indication of the laser's robustness about a specific point by noting the extent to which that location is isolated from the other attracting solutions found. As the gain is increased, the laser transitions from below threshold to Q-switched mode locking at $g_0 = 0.14$, and this region persists until $g_0 = 1.1$ where the laser enters a region of steady-state mode locking. As the gain is further increased, a coexisting attractor appears around $g_0 = 2.15$, and this state may be described as a steady-state mode-locked solution where the laser has two pulses simultaneously circulating within the cavity. Q-switched mode locking appears again above $g_0 = 2.65$, which is similar to the findings in [7]; however, using the forward history, we find the reemergence of a coexisting mode-locked state for $3.2 < g_0 < 3.45$. It is worth pointing out that this region of Q-switched mode locking disappears for linewidth enhancement factors below 0.25. A mode-locked state with three pulses is found above $g_0 = 3.6$, likewise above $g_0 = 3.27$, a state with four pulses exists. The CW background accompanying the four-pulse state (barely visible in Fig. 1) is due to incomplete relaxation of the absorber between subsequent optical pulses; this prevents realizing a state with more than four pulses for this cavity length unless the relaxation time is decreased and also makes the experimental realization of this state unlikely. Further increases in gain push the laser into a noisy region of oscillation with an increasing CW background. For values of $g_0 > 5.55$, the laser completely deteriorates into CW behavior although the forward history predicts the presence of an oscillatory state up till $g_0 = 6.38$. Although this figure does not capture all of the available states, it does reveal hysteresis, an effect frequently observed in passively mode-locked lasers [18].

One interesting observation is that this figure does not predict a region of traditional Q-switching. This has been commented on in the past and is related to the damping of the relaxation oscillations [7]. In this DDE model, it is related to the normalized round-trip time T; as this value is decreased, we find a region of classical Q-switching where pulses are emitted but at a rate far less than that of the cavity's free-spectral range.

Fig. 2 explores some of the previously noted regions by plotting the amplitude of the optical field in the various domains identified in the discussion of Fig. 1. Each figure clearly corresponds to a different state of operation. Because all of the results shown in this figure were generated through seeding the computation in the "backward" direction, the state consisting of three pulses is not shown.

Shifting our focus to fundamental mode locking, the intensity of the electric field and the carrier concentrations are plotted in Fig. 3, where $g_0 = 2.0$. This figure shows that the optical intensity is temporally asymmetric. Using this result and the analytic hyperbolic-secant solution admitted by many passively mode-locked solid-state lasers [19], the applicability of an unsymmetrized version of this pulse shape in fitting these results

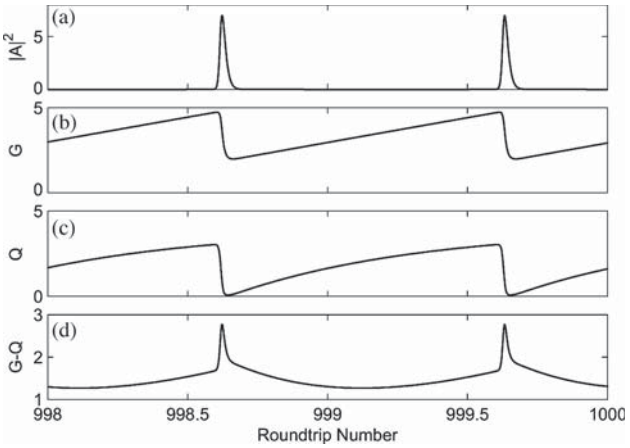

Fig. 3. (a) Optical intensity. (b) Carrier densities in the gain region. (c) Densities in the absorber region. (d) Difference between the carrier densities, which reveals the fast and slow components of the time-dependent gain. The parameters used are listed in Table I.

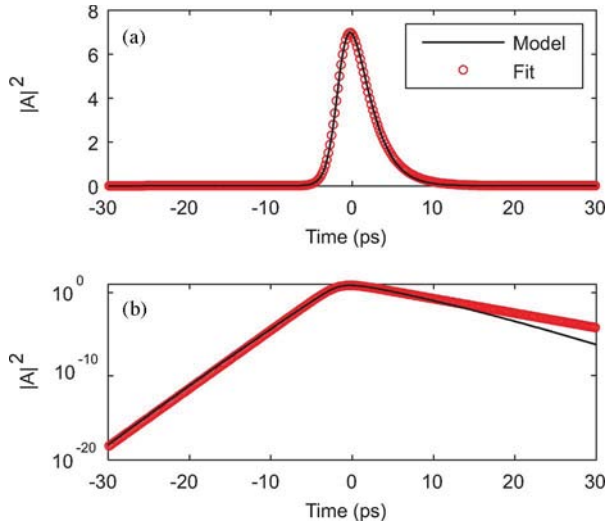

Fig. 4. Comparison between the numerical solution of (3)–(5) and the analytic fit given in (6). In this figure, the round-trip time has been scaled to 200 ps and the parameters used are listed in Table I.

was investigated in Fig. 4. Such an ansatz takes the form

$$|A(t)| = c_1 \frac{2}{e^{c_2(t-t_0)} + e^{-c_3(t-t_0)}} \tag{6}$$

where c_n and t_0 are coefficients. In Fig. 4, $c_1 = 2.18$ normalizes the peak intensity to 7.0, $c_2 = 0.2$ ps^{-1} characterizes the slope of the trailing edge of the pulse, $c_3 = 0.8$ ps^{-1} characterizes the slope of the leading edge of the pulse, and $t_0 = -1.65$ ps centers the fit about $t = 0$. Fig. 4 assumes that the laser operates at 5 GHz in order to convert the normalized round-trip time in the device to a physical timescale and facilitate the comparison. Although this pulse shape fits the intensity predicted by (3)–(5) very accurately about the pulse center, the agreement between the fit and the numerical results begins to diverge in the pulse wings. This splitting is attributed to the increased importance of the slow-stage component in the $G - Q$ relationship, as shown in Fig. 3. Of course, (6) collapses to the commonly used hyperbolic-secant pulse shape for $c_2 = c_3$; therefore, this general form should remain valid where mode locking is observed regardless of the symmetry.

IV. Device Description and Experimental Setup

In this paper, we experimentally characterized a two-section quantum-dot laser that was grown by elemental source molecular beam epitaxy on a (0 0 1) GaAs substrate following standard ridge waveguide laser processing. The self-assembled quantum dots were grown in compressively strained quantum wells. This so-called dots-in-a-well (DWELL) structure [1] uses the quantum wells to capture carriers, thus acting as a carrier bath (for the dots) that improves the dot's ability to capture carriers. The active region of the device investigated was composed of six DWELL layers, each separated by a 16-nm-thick GaAs barrier region, resulting in a total waveguide core thickness of 166 nm.

In the transverse direction, the laser had a ridge width of 3.5 μm while it was composed of two electrically isolated sections along the cavity length; a 1.0-mm region was biased by 4 V to act as a saturable absorber with a measured unsaturated absorption of 28 cm^{-1} at 1238 nm and a 7.3-mm region had 100 mA injected into it to serve as the gain medium with a measured gain at the operating wavelength of 4.8 cm^{-1}. The threshold current was 90 mA, and at 100 mA, which was the current used throughout the rest of this paper, only the ground state plays a role in performance; the first excited state, located around 1150 nm, remains well below threshold. Both facets were cleaved and then coated; the facet near the absorber was high-reflectivity coated ($R \approx 95\%$) while the other facet had an antireflective coating ($R \approx 5\%$).

To simplify handling and provide electrical isolation, the laser was mounted on AlN using indium. To insure stable mode locking over the time needed to acquire the experimental data, the laser assembly was then mounted on a copper block, again using indium. The temperature of the composite system was held at 20 °C by a thermoelectric cooler (which was contacted to the copper block using thermal grease) and driver (ILX LDC-3916). The two-section laser was electrically addressed using microprobes and the optical output of the laser was coupled into a polarization-maintaining single-mode optical fiber to facilitate placement issues associated with characterization. Although the laser output could have been collimated and relayed through free space directly into the associated diagnostic systems, the combination of a short 1-m fiber and the low peak power levels ensures that the fiber does not introduce any pulse distortion into the setup.

V. Experimental Results

An optical spectrum analyzer, autocorrelator, and a high-speed detector in conjunction with a microwave spectrum analyzer provided traditional pulse and pulse train characterization, and allowed us to quickly find a stable mode-locking region whose parameters were previously noted. This resulted in an optical spectrum with a 4.3-nm full-width at half-maximum (FWHM), as shown in Fig. 5. The satellite peak located at 1236 nm in this figure is evidence of the competition between

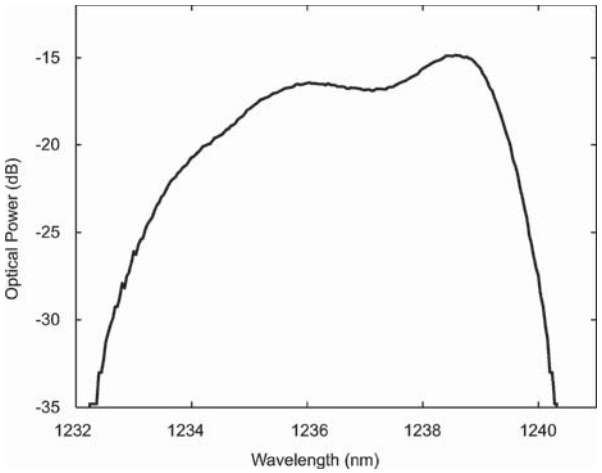

Fig. 5. Experimentally measured optical spectrum of our mode-locked pulse train indicates a spectral FWHM of 4.3 nm.

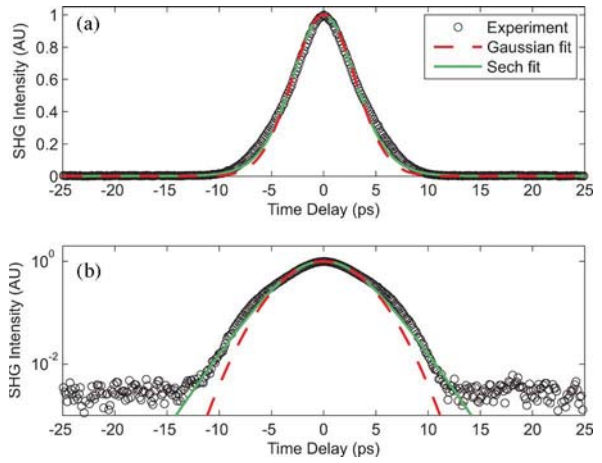

Fig. 6. Experimentally obtained SHG autocorrelation trace (circles) shown with a 5.1-ps FWHM Gaussian fit (dashed line) and a 4.9-ps FWHM hyperbolic secant fit (solid line); the FWHM of the actual field is 5.1 ps.

inhomogeneous and homogeneous broadening in the quantum-dot medium [10]; it is not related to the excited state of the quantum dots. Ultimately, these two peaks separate more clearly and cause the breakup of the pulse at higher bias currents as seen in [10]; however, in this figure, the two peaks are still coupled. Another notable feature shown in this figure is that the spectrum appears to gradually rise on its short-wavelength side whereas the long-wavelength tail drops rapidly resulting in an asymmetric optical spectrum. This is also thought to be due to the different broadening mechanisms having different gain spectra.

As seen in Fig. 6, the autocorrelation trace of the mode-locked pulses has a 7.2-ps FWHM that corresponds to 5.0-ps or 4.58-ps pulses assuming a Gaussian or hyperbolic-secant pulse shape, respectively. Fig. 6 also reveals that neither fit is accurate, although the hyperbolic-secant pulse shape provides better agreement with the data on the pulse wings. The autocorrelation result also indicates that the pulses are $\sim 12\times$ their transform limit (assuming a hyperbolic-secant pulse shape). Finally, the microwave spectrum analyzer was used to indicate the presence

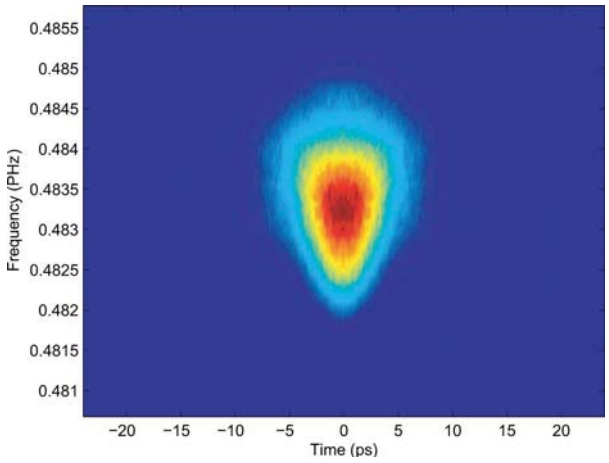

Fig. 7. Experimentally measured FROG spectrogram.

of mode locking and identified that the laser's repetition rate was 5 GHz.

To resolve some of the outstanding issues raised by these figures, such as the discrepancy between pulse shapes and the large time–bandwidth product, we constructed a highly sensitive FROG system that would provide useful data in spite of the low SNR available. The FROG system had a standard configuration and consisted of a temporal delay line that performed a traditional noncollinear type-I autocorrelation using a 1-mm-thick $LiIO_3$ crystal. The output of the autocorrelator was spectrally gated, using a 1200 lines/mm grating monochromater with a 0.2-nm resolution, before being detected by a sensitive photomultiplier tube (Hamamatsu R955). The resulting electronic signal was low-pass filtered, and then amplified using a low-noise current preamplifier (SRS SR570). This setup allowed us to obtain the spectrogram shown in Fig. 7, which indicates the existence of a mode-locked pulse and whose triangular shape immediately confirms that these pulses are chirped.

Using the data from Fig. 7 in the standard FROG phase-retrieval algorithm [20] results in the normalized intensity shown by the solid (black) traces in Fig. 8(a) and (b) on a linear and logarithmic scale, respectively. Fig. 8 reveals pulse asymmetry that is obscured in any autocorrelation measurement and hidden in the spectrogram of Fig. 7. In contrast to the intensity, the optical phase retrieved from the FROG spectrogram was overwhelmingly symmetric to the extent that it was accurately fit by the parabola $\phi(t) = 0.55t^2$, where t is the time in picoseconds and $\phi(t)$ is the phase in radians. The measurement of a symmetric phase despite the asymmetric pulse shape is most likely caused by a nonlinear effect and is currently under investigation [8].

As a consequence of the pulse asymmetry, the field is poorly fit by both Gaussian and hyperbolic-secant functions. Nevertheless, the unsymmetrized hyperbolic-secant of (6) provides a good fit, as shown in Fig. 8(a) and (b). The agreement between the extracted amplitude and (6) is favorable over the pulse's entire leading edge to the extent it can be commented on due to the SNR. During the trailing edge of the pulse, it appears that the carrier dynamics following the closing of the gain window (in the "slow stage" region) play an increased role in mediating

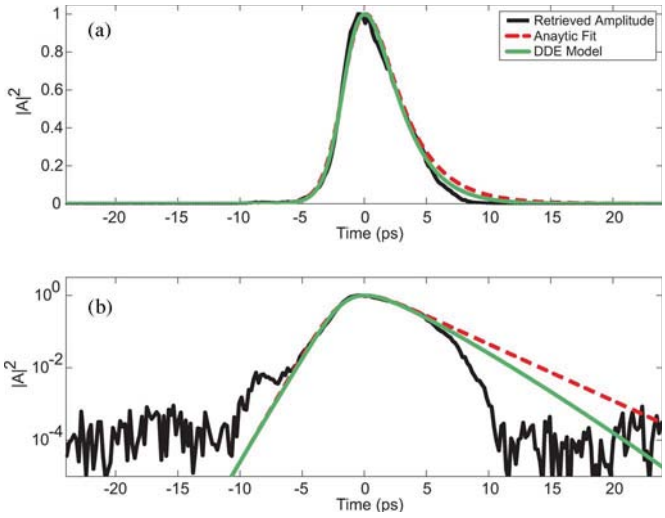

Fig. 8. (a) Retrieved electric-field intensity (solid black), the electric-field intensity predicted by our fit (dashed line), and the intensity predicted by our model (gray). (b) Same as (a). However, the data are shown here on a semilogarithmic plot.

the field and the fit retains its accuracy over a restricted window up to 5 ps only. The asymmetric pulse shape also places an increased importance on resolving the time ambiguity inherent in the second-harmonic generation based FROG measurement. Although the parabolic phase indicates that the pulses should be compressible via optical fiber, attempts to realize this have only lead to pulse broadening. This result, coupled with our opinion that the differential absorption is much larger than the differential gain [10], provides strong evidence that the time axis orientation reported in this paper is correct.

The results obtained by solving (3)–(5) using the values found in Table I are also shown in Fig. 8. The comments on their accuracy are identical to those previously made concerning the analytic fit; however, the agreement during the trailing edge of the pulse is slightly better. The improvement is due to the model's incorporation of the carrier dynamics during the slow stage although the experimental results indicate that these are more complicated than assumed by the DDE model. Although the model used in this paper did not include the full dynamics associated with the carrier capture in the wells, and then subsequent capture by the dots, it was able to produce fairly accurate results. As noted in Section II, a more thorough treatment of the carriers has been done for devices containing wetting layers [16], [17]. Although the same tact could be taken with these DWELL devices, the likelihood of a nonuniform response across all DWELL regions complicates matters (they are in series and so repopulation may be delayed in the different layers); the lack of compelling experimental evidence, the low SNR of the data, and the good general agreement between the model and data justified the decision to investigate the applicability of the model used.

Although the experimentally extracted phase was predominantly symmetric, the phase predicted by the DDE model was asymmetric. This discrepancy, thought to be related to a nonlinear dependence of the linewidth enhancement factor, is currently under investigation. This should also explain the model's prediction of an almost transform-limited pulse.

VI. Conclusion

In this paper, a system of DDEs was used to form a simple model to explore different regions of operation in a two-section quantum-dot laser. By focusing on fundamental mode locking, an asymmetric hyperbolic-secant function was found to agree well with the numerical results in the vicinity of the pulse center. Experimentally, a two-section quantum-dot laser was investigated using traditional measurement diagnostics. More importantly, however, a FROG system was constructed and used to directly measure the electric field outside of a mode-locked quantum-dot laser, and compared with a DDE model for what we believe to be the first time. The realization of significant pulse asymmetry does not preclude the possibility of symmetric pulses out of these lasers, however, it does provide a strong argument for the utility of electric-field reconstruction techniques in the characterization of pulses from these lasers. Finally, the results from the numerical simulation were overlayed on the experimental data and good agreement was found for the pulse amplitude.

References

[1] G. T. Liu, A. Stintz, H. Li, K. J. Malloy, and L. F. Lester, "Extremely low room-temperature threshold current density diode lasers using InAs dots in $In_{0.15}Ga_{0.85}As$ quantum well," *Electron. Lett.*, vol. 35, pp. 1163–1165, 1999.

[2] Y.-C. Xin, V. Kovanis, A. L. Gray, L. Zhang, and L. F. Lester, "Reconfigurable quantum dot monolithic multisection passive mode locked lasers," *Opt. Exp.*, vol. 15, pp. 7623–7633, 2007.

[3] T. C. Newell, D. J. Bossert, A. Stintz, B. Fuchs, K. J. Malloy, and L. F. Lester, "Gain and linewidth enhancement factor in InAs quantum-dot laser diodes," *IEEE Photon. Tech. Lett.*, vol. 11, no. 12, pp. 1527–1529, Dec. 1999.

[4] R. Debusmann, T. W. Schlereth, S. Gerhard, W. Kaiser, S. Höfling, and A. Forchel, "Gain studies on quantum-dot lasers with temperature-stable emission wavelength," *IEEE J. Quantum Electron.*, vol. 44, no. 2, pp. 175–181, Feb. 2008.

[5] H. Wang, A. R. Rae, M. G. Thompson, R. V. Penty, I. H. White, and A. R. Kovsh, "Dynamic switching of a 10 GHz quantum dot mode-locked laser using an integrated quantum dot switch," in *Proc. IEEE Int. Conf. Photon. Switching*, Aug. 2007, pp. 113–114.

[6] E. U. Rafailov, M. A. Cataluna, and W. Sibbett, "Mode locked quantum-dot lasers," *Nat. Photon.*, vol. 1, pp. 395–401, 2007.

[7] E. A. Viktorov, P. Mandel, M. Kuntz, G. Fiol, D. Bimberg, A. G. Vladimirov, and M. Wolfrum, "Stability of the mode locked regime in quantum dot lasers," *Appl. Phys. Lett.*, vol. 91, pp. 231116-1–231116-3, 2007.

[8] F. Grillot, B. Dagens, J.-J. Provost, H. Su, and L. F. Lester, "Gain compression and above-threshold linewidth enhancement factor in 1.3-μm InAs-GaAs quantum-dot lasers," *IEEE J. Quantum Electron.*, vol. 44, no. 10, pp. 946–951, Oct. 2008.

[9] N. G. Usechak, Y. Xin, L. F. Lester, D. J. Kane, and V. Kovanis, "Modeling and direct electric-field measurements of passively mode locked quantum-dot lasers," presented at the CLEO, 2008, San Jose, CA, Paper CThF2..

[10] Y.-C. Xin, D. J. Kane, and L. F. Lester, "Frequency-resolved optical gatin characterisation of passively modelocked quantum-dot laser," *Electron. Lett.*, vol. 44, pp. 1255–1257, 2008.

[11] B. Resan, L. Archundia, and P. J. Delfyett, "FROG measured high-power 185-fs pulses generated by down-chirping of the dispersion-managed breathing-mode semiconductor mode locked laser," *IEEE Photon. Technol. Lett.*, vol. 17, no. 7, pp. 1384–1386, Jul. 2005.

[12] A. G. Vladimirov and D. Turaev, "A new model for a mode-locked semiconductor laser," *Radiophys. Quantum Electron.*, vol. 47, pp. 769–776, 2004.

[13] A. G. Vladimirov and D. Turaev, "Model for passive mode locking in semiconductor lasers," *Phys. Rev. A*, vol. 72, pp. 033808-1–033808-13, 2005.
[14] R. L. Davidchack, Y.-C. Lai, A. Gavrielides, and V. Kovanis, "Regular dynamics of low-frequency fluctuations in external cavity semiconductor lasers," *Phys. Rev. E*, vol. 63, pp. 056206-1–056206-6, 2001.
[15] T. Erneux, L. Larger, M. W. Lee, and J.-R. Goedgebuer, "Ikeda Hopf bifurcation revisited," *Phys. D*, vol. 194, pp. 49–64, 2004.
[16] T. W. Berg and J. Mørk, "Quantum dot amplifiers with high output power and low noise," *Appl. Phys. Lett.*, vol. 82, pp. 3083–3085, 2003.
[17] E. A. Viktorov, P. Mandel, A. G. Vladimirov, and U. Bandelow, "Model for mode locking in quantum dot lasers," *Appl. Phys. Lett.*, vol. 88, pp. 201102-1–201102-3, 2006.
[18] K. Tamura, E. P. Ippen, H. A. Haus, and L. E. Nelson, "77-fs pulse generation from a stretched-pulse mode locked all-fiber ring laser," *Opt. Lett.*, vol. 18, pp. 1080–1082, 1993.
[19] H. A. Haus, "Theory of mode locking with a fast saturable absorber," *IEEE J. Sel. Topics Quantum Electron.*, vol. 6, no. 6, pp. 1173–1185, Nov./Dec. 2000.
[20] D. J. Kane and R. Trebino, "Characterization of arbitrary femtosecond pulses using frequency-resolved optical gating," *IEEE J. Quantum Electron.*, vol. 29, no. 2, pp. 571–579, Feb. 1993.

Nicholas G. Usechak (M'06) was born in Long Branch, NJ, in 1976. He received two B.S. degrees (Hons.) in electrical engineering and engineering physics from Lehigh University, Bethlehem, PA, in 2000, and the M.S. and Ph.D. degrees in optical engineeringfrom the Institute of Optics, University of Rochester, Rochester, NY, in 2003 and 2006.

During 1999–2000, he was a Presidential Scholar at Lehigh. He was a Frank J. Horton Fellow at the University of Rochester. For one year, he was with Trumpf Photonics, Cranbury, NJ, where he was engaged in the characterization of high-power semiconductor laser arrays, automating experiments, and modeling the thermal effects of solder interfaces using transient temperature-extraction experiments to ground those models. He then joined the Air Force Research Laboratory, Wright–Patterson Air Force Base, Dayton, OH, where he is engaged in research on mode-locked semiconductor lasers. His current research interests include nonlinear fiber optics, fiber lasers, ultrafast optics, high-speed test and measurement, high-power semiconductor lasers, and mode-locked semiconductor lasers.

Dr. Usechak is a member of the Optical Society of America (OSA), Tau Beta Pi, and Sigma Xi.

Yongchun Xin (S'03–M'05) received the B.S. and M.S. degrees in physics from Peking University, Beijing, China, in 1996 and 1999, respectively, and the M.S. degree in electrical engineering and the Ph.D. degree in optical science from the University of New Mexico (UNM), Albuquerque, in 2002 and 2006, respectively.

He was engaged in research on device physics, and fabrication and characterization of semiconductor quantum-dot light emitters that include mode-locked laser and superluminescent diodes. From 2007 to August 2008, he was a Postdoctoral Scholar at the Center of High Technology Materials, UNM. He is currently with IBM Systems and Technology Group, Semiconductor Solutions, Armonk, NY. His current research interests include novel long-wavelength mode-locked laser, terahertz generation and sensing, and the high-sensitivity and high-resolution frequency-resolved optical gating (FROG) system.

Chang-Yi Lin (S'08) received the B.S. degree in physics from the National Cheng Kung University, Tainan, Taiwan, in 2004. He is currently working toward the Ph.D. degree in optical science and engineering at the University of New Mexico (UNM), Albuquerque.

His current research interests include device physics, fabrication and characterization of semiconductor quantum-dot lasers, especially in novel long-wavelength mode-locked lasers, and improving the conversion efficiency of microwave generation through passively mode-locked lasers.

Luke F. Lester (S'89–M'91–SM'01) received the B.S. degree in engineering physics and the Ph.D. degree in electrical engineering from Cornell University, Ithaca, NY, in 1984 and 1992, respectively.

He was an Engineer at the General Electric Electronics Laboratory, Syracuse, NY, where he was engaged in research on high-electron-mobility transistors for millimeter-wave applications. He was a Co-Founder and the Chief Technology Officer of Zia Laser, Inc., a startup company using quantum-dot laser technology to develop products for communications and computer/microprocessor applications. He was an US Air Force Summer Faculty Fellow in 2006 and 2007. He is currently a Professor in the Department of Electrical and Computer Engineering, University of New Mexico (UNM), Albuquerque, where he is also the Microelectronics Endowed Chair Professor and an Associate Director of the Center for High Technology Materials. He has over 20 years of experience in III–V semiconductor materials and devices. His current research interests include quantum dot lasers, mode locking, injection locking, quantum dot solar cells, and III-V semiconductor processing. He has authored or coauthored more than 80 articles published in various journals and more than 100 papers presented at various conferences.

Prof. Lester is an active organizer of the Lasers and Electro-Optics Society (LEOS) conferences, workshops, and journals. He was the recipient of the 1998 UNM School of Engineering Research Award, the 1994 Martin Marietta Manager's Award, and the 2007 UNM Electrical and Computer Engineering (ECE) Teaching Award.

Daniel J. Kane (M'00) received the B.S. degree from Montana State University, Bozeman, in 1983, and the M.S. and Ph.D. degrees from the University of Illinois at Urbana-Champaign, Urbana-Champaign, in 1995 and 1989, respectively, all in physics.

He was the Founder and President of Mesa Photonics, LLC. He was a Postdoctoral Fellow at the Los Alamos National Laboratories. In 1992, he joined Southwest Sciences, Inc., Santa Fe, NM, where he is currently a Principal Research Scientist He has over 15 years of experience in the development of ultrafast laser pulse measurement techniques and is the Co-Inventor of frequency-resolved optical gating (FROG). He is also the Inventor of the principal components generalized projections (PCGP) algorithm, a very fast phase retrieval algorithm for the measurement of ultrafast laser pulses. He has authored or coauthored papers in spectroscopy and has developed a method to mathematically remove etalon fringes from wavelength modulation spectra. He holds ten patents and has two patents pending. His current research interests include optical coherence tomography and nonlinear optics.

Dr. Kane is a Fellow of the Optical Society of America (OSA) and a member of Sigma Xi.

Vassilios Kovanis received the Degree in physics from the University of Athens, Athens, Greece, a Graduate degree from Temple University, Philadelphia, PA, and the Ph.D. degree from the University of New Mexico, Albuquerque, in condensed matter theory.

In September 1989, he joined the Nonlinear Optics Center, Air Force Weapons Laboratory, Kirtland Air Force Base, where for 11 years, he was engaged in research on multiple projects in optical and electronic technologies. He held research faculty positions in the Departments of Applied Mathematics and Electrical Engineering, University of New Mexico. From 1992 to 1994, he was a National Research Council Fellow. He was a Senior Research Scientist at the Corporate Research and Development Laboratories, Corning, Inc., Corning, NY, where he was managing technical interactions with telecommunications system houses. He was also with BinOptics Corporation, Ithaca, NY, as a Program Manager for next-generation photonic product development. From 2003 to 2005, he was a Faculty Member in the Department of Applied Mathematics, Rochester Institute of Technology. He returned to the Air Force Research Laboratory in June 2005. He is currently with the Photonics Technologies Branch, Sensors Directorate of the Air Force Research Laboratory, Wright–Patterson Air Force Base. His research interests are in optical injection locking, coherence collapse, optical coupling of semiconductor lasers, as well as controlling, synchronizing, and communicating with chaotic waveforms.